

# Characterization of UV-Induced Graft Polymerization of Poly(acrylic acid) Using Optical Waveguide Spectroscopy

Li-Qiang Chu,<sup>†,‡</sup> Wee-Jin Tan,<sup>§</sup> Hai-Quan Mao,<sup>⊥,§</sup> and Wolfgang Knoll<sup>\*,†,‡</sup>

Max-Planck-Institut für Polymerforschung, Ackermannweg 10, 55128, Mainz, Germany; Departments of Material Science and Engineering and of Chemistry, National University of Singapore, 117543, Singapore; Division of Biomedical Science, Johns Hopkins in Singapore, Singapore 138669, Singapore; and Department of Materials Science and Engineering and Whitaker Biomedical Engineering Institute, Johns Hopkins University, 102 Maryland Hall, 3400 N. Charles Street, Baltimore, Maryland 21218

Received March 13, 2006; Revised Manuscript Received August 13, 2006

**ABSTRACT:** UV-induced graft polymerization is a simple and effective method for the surface modification and functionalization of polymeric materials. The structure of poly(acrylic acid) (PAAc) grafted onto a polymeric surface by UV-induced graft polymerization of acrylic acid was investigated using optical waveguide spectroscopy (OWS). The PAAc graft layer exhibited a large increase in thickness in water compared to that in the dry state due to the swellability of the PAAc chains. Its thickness further increased with increasing the pH of the aqueous solution. This could be attributed to the increased electrostatic repulsion of the carboxylate anions on the PAAc chains, as the ionization degree of the carboxylic groups increases with pH. The thickness of the PAAc graft layer is dependent on the graft condition employed, including the UV intensity and irradiation time, and the AAc monomer concentration. On the basis of these data, we propose a model for the structure of the PAAc graft layer and a PAAc layer modified by galactose ligands.

## Introduction

Surface graft polymerization<sup>1–8</sup> has attracted considerable interest as a simple and versatile approach to introduce functional groups, such as carboxyl, epoxide, amine, or hydroxyl groups, onto a variety of polymeric substrates. To initiate the graft polymerization, various energy sources have been investigated including  $\gamma$ -ray, electron beam, ultraviolet irradiation, low-temperature plasma, and ozone treatment. The UV-induced graft polymerization is attractive because of its simplicity and low cost. The graft layer is stable due to the covalent binding, while the bulk properties of the polymer remain unchanged.

Acrylic acid (AAc) has been widely used in graft polymerization reactions for introducing carboxyl groups in a large number of different applications.<sup>9–11</sup> The grafted poly(acrylic acid) (PAAc) chains can be utilized to further react with biomolecules through covalent linkages. Recently, galactosylated PET surfaces were successfully prepared by coupling a galactose ligand to the PAAc graft chains and were employed as substrates for rat primary hepatocyte cultures.<sup>12,13</sup> It was found that the galactosylated surfaces not only allowed for efficient hepatocyte attachment mediated by specific binding between galactose ligand and the asialoglycoprotein receptor on the hepatocyte surface but also promoted spheroid formation of the attached cells because of the high surface density of the galactose ligands on the substrate. The ligand and graft chain mobility are likely main factors influencing the ligand accessibility to cells and hence affect cell adhesion, migration, and functions. The present study was motivated by the need to investigate the structure of the grafted galactosylated PAAc chains, aiming at providing

an in-depth correlation between substrate surface morphology and cellular behavior.

The structure of polymers grafted on a surface is dependent on the graft density, the chain length, and the environment in contact with the grafted layer.<sup>1,2</sup> In a good solvent environment, the grafted chains at high density will stretch away from the surface, forming a polymer brush. In a poor solvent, the grafted chains will collapse. Experimental studies have demonstrated that grafted PAAc chains exhibit different structures depending on the solvent, the pH value, and the ionic strength of the contacting medium. Many techniques have been employed to explore the structure of the graft layer, including atomic force microscopy (AFM),<sup>14,15</sup> surface plasmon resonance spectroscopy,<sup>16</sup> zeta potential measurements,<sup>17</sup> etc.

In this work, another optical technique, optical waveguide spectroscopy (OWS), was utilized to investigate the structure of UV-induced graft PAAc layer in air and in a liquid environment. The use of OWS for the characterization of polymer thin films has been described in detail elsewhere.<sup>18,19</sup> OWS can determine the refractive index ( $n$ ) and the thickness ( $d$ ) of a coating simultaneously, provided at least two modes can be guided in the thin film structure. It was applied successfully to monitor the swelling of polymer brushes.<sup>20,21</sup> A thin poly-(terephthalate-*co*-phosphate) (PTPP) film was spin-coated onto a substrate to a thickness of  $\sim 500$  nm and was used as the waveguide layer for the excitation of two waveguide modes and as the substrate for the UV-induced graft polymerization of AAc. The thickness of PAAc graft layer in the dry state and in a liquid solution was determined by OWS measurements. Finally, a galactosylated sample was prepared through the coupling of galactose ligands to the grafted PAAc layer, and its thickness was compared with that of the bare PAAc layer.

## Experimental Section

**Materials and Substrates.** Acrylic acid (AAc) and galactose were obtained from Merck Chemical Co. of Darmstadt, Germany.

\* To whom correspondence should be addressed; Tel (+49) 6131 379161; Fax (+49) 6131 379360; e-mail knoll@mpip-mainz.mpg.de.

<sup>†</sup> Max-Planck-Institut für Polymerforschung.

<sup>‡</sup> National University of Singapore.

<sup>§</sup> Johns Hopkins in Singapore.

<sup>⊥</sup> Johns Hopkins University.

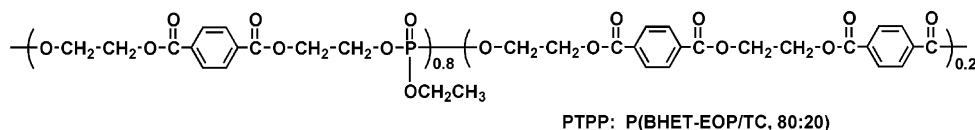


**Figure 1.** Chemical structure of poly(terephthalate-co-phosphate).

AAc was purified by distillation under reduced pressure. *N*-Hydroxysuccinimide (sulfo-NHS) was supplied by Pierce Chemical Co. of Rockford, IL. 1-Ethyl-3-(3-(dimethylamino)propyl)carbodiimide hydrochloride (EDC) was obtained from Sigma-Aldrich. The galactose ligand, 1-*O*-(6'-aminoheptyl)-D-galactopyranoside (AHG), was synthesized according to the method described previously.<sup>22</sup> The synthesis of poly(terephthalate-*co*-phosphate) (PBHET-EOP/TC, 80:20) was described in a previous paper,<sup>23</sup> which is referred to as PTPP in this report. Its chemical structure is given in Figure 1. Milli-Q water was used throughout the experiments. LaSFN9 glass slides ( $n = 1.844$  at  $\lambda = 633$  nm, Hellma Optik, Jena, Germany) were used in the OWS measurements. 2 nm chromium and 50 nm gold were evaporated onto the glass slide. Here the chromium layer is used to enhance the adhesion of gold on the LaSFN9 glass.

**Spin-Coating of PTPP onto Au-Coated LaSFN9.** The PTPP polymer dissolves in chloroform at 2 wt %, which was then spun at 2000–3000 rpm onto Au-coated LaSFN9 slides with a thickness of 400–600 nm. The substrates are referred to as PTPP/Au/LaSFN9. Prior to the OWS measurements, the films were dried at 50 °C for 24 h in order to remove any remaining solvent in the film.

**UV-Induced Graft Polymerization of AAc on the PTPP/Au/LaSFN9.** The PTPP/Au/LaSFN9 substrates were immersed in 220 mL of an aqueous AAc solution in a flat-bottom glass container. The AAc solution was deoxygenated thoroughly with Ar for 30 min and then sealed under an Ar atmosphere using a polyethylene film. The concentrations of the AAc solutions varied from 0.5% to 4%. The temperature of the reaction solution was maintained below 10 °C by cooling the container in an ice–water bath. The reaction mixture was then exposed to UV radiation (Dymax 5000-EC,  $\lambda = 320\text{--}390$  nm, Frankfurt, Germany) for 15 min. The UV power density on the substrate surface was 460 mW/cm<sup>2</sup> measured by a UV power meter (Model: TQ8210, Advantest, Tokyo, Japan). After graft polymerization, the substrate was washed exhaustively with  $5 \times 10^{-4}$  M NaCl solution and Milli-Q water in order to remove any monomer and homopolymer adsorbed on the surface. The resulting multilayer samples are referred to as PAAC–PTPP.

**Coupling of Galactose Ligands to the PAAC Graft Layer.** PAAC-PTPP/Au/LaSFN9 substrates were immersed into 5.0 mL of 0.1 M sodium phosphate buffer (pH = 8) with 5 mg of AHG, 5 mg of sulfo-NHS, and 50 mg of EDC. The mixture was gently shaken overnight. 50 mg of EDC was added to the solution every 24 h for two more days. After this reaction, the mixture was aspirated, and 1 mL of 0.1 M HCl was added to the well in order to quench the reaction. The sample was then washed with Milli-Q water. The obtained surface is referred to as Gal-PAAC-PTPP.

**OWS Measurements.** OWS measurements were carried out with a home-built setup based on the Kretschmann configuration (as shown in Figure 2) described before.<sup>19,21</sup> The OWS curve can be fitted using Fresnel equations yielding not only the refractive index  $n$  but also the thickness  $d$  of the film provided that at least two optical waveguide modes can be excited. The excitation of guided modes can be achieved not only by p-polarized light but also using s-polarized light. The samples were mounted to different Teflon cells: one for measurement in air with controlled humidity and one for liquid solutions with different pH values. Zero percent relative humidity was obtained by drying the samples over potassium hydroxide pellets for 30 min. To investigate the effect of the graft conditions on the thickness of the PAAc layer, the UV-induced graft polymerization was performed directly in the OWS setup (Figure 2). Quartz was used as the backside of the flow cell in order to minimize UV absorption. The LC5 UV spot light source (model: L8222-01,  $\lambda = 300\text{--}450$  nm, Hamamatsu Photonics K.K. Japan), which allows for a fine control of the UV output and the

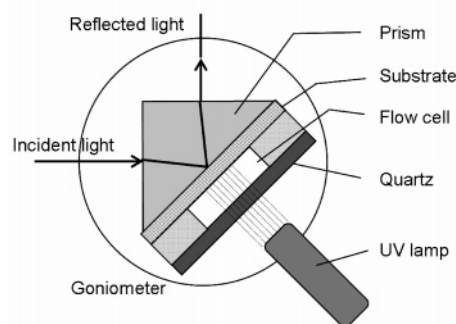


**Figure 2.** Diagram illustrating the flow cell and sample arrangement in OWS coupled with a UV spot light source.

irradiation time, was employed to initiate graft polymerization. The AAc solution was introduced into the cell and then bubbled for 5 min with Ar in order to remove dissolved oxygen, which is well-known to act as an inhibitor for free-radical-initiated polymerization. During UV irradiation, the change in thickness was monitored by measuring the shift of the minimum dip of a waveguide mode as a function of time. The time resolution is better than 1.5 s. After UV irradiation, an OWS angular scan was carried out in order to determine the thickness and the refractive index of the polymers.

## Results and Discussion

### Effect of UV Irradiation on the Thickness of PTPP Layer.

Polymers exposed to UV irradiation have been demonstrated to undergo different surface (and bulk) reactions, such as photooxidation, photodegradation, or photoablation, depending on the intensity and wavelength of the UV light, as well as the sensitivity of the polymer to UV light. The PTPP was used as a substrate for UV-induced graft polymerization in this study. The UV spot light source employed has a wavelength ranging from  $\lambda = 300\text{--}450$  nm and allows for a fine control of the intensity. The effect of this UV irradiation on the PTPP substrate was first determined experimentally. For this purpose, a PTPP thin film was spun onto an Au/LaSFN9 slide with a thickness sufficient for the excitation of at least two waveguide modes. OWS spectra were then scanned in water with both p- and s-polarized light, as shown in Figure 3. Two waveguide modes could be excited: one for p-polarized light (curve a1) and another one for s-polarized light (curve a2). Next, the PTPP was exposed to UV irradiation for 10 min, and the OWS spectra were recorded again (curves b1 and b2). The thickness and the refractive index of PTPP thus could be obtained from a fitting based on Fresnel's equations. The results indicated that the PTPP thickness before UV irradiation was  $d = 541.5$  nm and was reduced to  $d = 421.5$  nm after 10 min UV irradiation. The refractive index of PTPP remained unchanged,  $n = 1.510$ , indicating that UV irradiation resulted in the photoablation of PTPP.

The change in PTPP thickness during UV irradiation was monitored in real time by measuring the shift of the minimum dip of a waveguide mode as a function of time, as shown in the inset of Figure 3. The waveguide mode continued shifting to low angles as the UV irradiation continued, indicating that the thickness of PTPP layer gradually decreased due to UV irradiation. The angle shift and the decrease of the PTPP

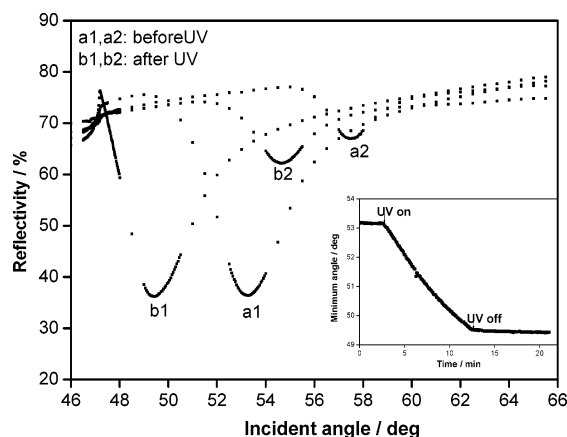


**Figure 3.** OWS spectra of a  $d = 541.5$  nm thick (in water) PTPP upon UV irradiation. Both p- and s-polarized OWS were measured for the PTPP layer before and after UV irradiation. a1, b1: p-polarized; a2, b2: s-polarized. (UV intensity:  $460 \text{ mW/cm}^2$ ). The inset shows the change of the position of the waveguide mode in a1 during UV irradiation. The angle shift and the decrease in the PTPP thickness with time follows a linear relationship. The corresponding thickness decreases from  $d = 541.5$  to  $d = 421.5$  nm.

thickness followed a linear relationship with time, which suggests that the UV-induced ablation of PTPP layer depends only on the exposure time for a given UV spectrum and power density. As our fitting program is based on Fresnel's equations and assumes a multilayer structure,<sup>19,24</sup> the decrease of the PTPP thickness due to UV exposure must be taken into account in the fitting for the thickness of subsequently grafted and modified layers.

**PAAc Graft Layer in the Dry State and in Water.** The UV-induced graft polymerization of AAc on PTPP layers was carried out using the same protocol as reported previously.<sup>12,13</sup> Spin-coating of PTPP was achieved with high reproducibility; the standard deviation of the thickness of the several PTPP layers is below 3% (from six samples). One of the PTPP substrates was used as a reference for OWS measurements, and other PTPP substrates were used for UV-induced graft polymerization of AAc with monomer concentrations ranging from 0.5 to 4%. After the graft polymerization, the substrates were washed extensively with water in order to remove residual homopolymer adsorbed on the surface and then dried in an oven at  $T = 50^\circ\text{C}$ . The thickness of the dry PAAc graft layer was measured using OWS in a cell with 0% relative humidity. Typical p-polarized OWS spectra for both PTPP and PAAc-PTPP, respectively, are shown in Figure 4A. Two waveguide modes were excited for PTPP, from which the thickness and the refractive index of the PTPP layer could be determined. The data were also confirmed by s-polarized OWS results (data not shown). PAAc grafted onto PTPP also resulted in two waveguide modes in its OWS spectrum. As can be seen from Figure 4A, both modes shift to higher angles compared to those of the bare PTPP substrate, suggesting an increase in thickness due to the grafted PAAc chains.

Regarding the fitting of the OWS for the PAAc-PTPP system based on Fresnel's equations, a two-layer model was employed: the PAAc graft layer was regarded as a new layer, while the PTPP substrate was assumed to have a reduced thickness due to the UV ablation discussed above. The relative extent of the two layers is not clear, and of course, there could be an interface layer between the UV ablated substrate and the PAAc grafted chains. Here we treat the sample as a model with two uniform layers and assume the thickness of the PTPP substrate to be reduced by 120 nm due to UV irradiation, as indicated in

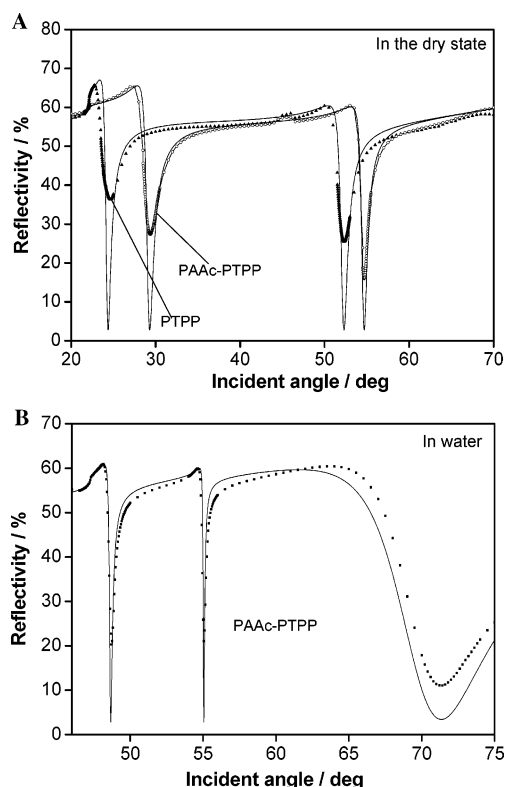


**Figure 4.** (A) OWS spectra (p-polarized) of the PTPP substrate (▲) and the PAAc-PTPP layers (○) in the dry state. PAAc grafting was characterized by the angular shift of the waveguide modes. (B) OWS spectrum (p-polarized) of the PAAc-PTPP in  $\text{H}_2\text{O}$ . The dip at  $\theta = 71.3^\circ$  is the SPR mode, which in present case (PTPP thickness  $> 300$  nm) is related to the refractive index of PTPP substrate only. The solid lines are the calculated reflection curves obtained from Fresnel equations. Graft conditions: 0.5% AAc; UV:  $460 \text{ mW/cm}^2$ , 10 min.

**Table 1. Thickness and Refractive Index of PTPP and PAAc Layers Grafted on a PTPP Surface from Different AAc Concentrations**

|                            | in the dry state   |                    | in water         |                  |
|----------------------------|--------------------|--------------------|------------------|------------------|
|                            | thickness (nm)     | refractive index   | thickness (nm)   | refractive index |
| PTPP                       | 543.5              | 1.541              | 581              | 1.530            |
| PTPP after UV <sup>a</sup> | 423.5 <sup>b</sup> | 1.541 <sup>c</sup> | 461 <sup>b</sup> | — <sup>d</sup>   |
| PAAc (0.5% AAc)            | 182                | 1.528              | 671              | 1.451            |
| PAAc (2% AAc)              | 514                | 1.528              | 1370             | 1.446            |
| PAAc (4% AAc)              | 574                | 1.527              | — <sup>e</sup>   | — <sup>e</sup>   |

<sup>a</sup> Data were used for OWS spectra fitting of the PAAc graft layer. <sup>b</sup> All thicknesses were assumed to decrease by  $\Delta d = 120$  nm due to UV ablation at the given conditions. <sup>c</sup> The refractive index was assumed to remain constant for the dry film. <sup>d</sup> In water, the refractive index of PTPP is derived from the SPR mode. <sup>e</sup> Data could not be obtained due to the delamination of the polymer film from the Au substrate.

Figure 3. The results thus obtained for the PAAc coating prepared at different AAc concentrations are summarized in Table 1. With increased concentration of AAc, the dry thickness of the grafted layer increases. These results are in good agreement with the literature.<sup>12</sup>

It has been shown that PAAc chains stretch out in an aqueous solution and assume an extended conformation.<sup>16</sup> Figure 4B shows a typical p-polarized optical waveguide spectrum of the grafted PAAc layer in water. As expected, the thickness of PAAc in water is much higher than that in the dry state (Table 1). These results can be explained by the fact that the PAAc is soluble in water. The PAAc chains exist in a stretched conformation. In contrast, PAAc chains collapsed in the dry state. When water molecules penetrate into the "fully hydrated PAAc layer", the overall refractive index of the polymer will



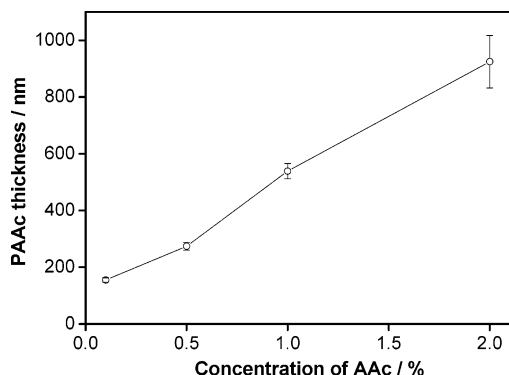


**Figure 5.** Effect of the AAc concentration on the thickness of the grafted PAAc layer prepared in OWS setup. The PAAc layer is in contact with aqueous AAc solution. Grafting conditions: 10 min UV of 460 mW/cm<sup>2</sup>.

decrease because the refractive index of water ( $n = 1.33$ ) is lower than that of the polymer (typically  $n \approx 1.5$ ). For example, the PAAc layer prepared with 2% AAc monomer exhibited a lower refractive index when immersed into water (from  $n = 1.528$  to 1.446). The thickness of PAAc prepared with 4% AAc could not be measured in water because the whole PAAc–PTPP sandwich detached from the Au substrate. This may be ascribed to the stress induced by the swelling of the PAAc. Water molecules penetrate into the PAAc chains when the substrate is incubated in water. The structural changes in the PAAc induced considerable stress inside the film, which is large for thicker PAAc layers, and caused the delamination of the PTPP from the metal substrate.

The present OWS setup is identical to a surface plasmon resonance spectrometer (SPR).<sup>19</sup> SPR employs an evanescent wave excited at a metal/dielectric interface, which propagates along the  $x$ -direction of this interface as a damped oscillatory wave.<sup>24</sup> It is interesting to notice that the SPR mode was observed at the high angle position in Figure 4B. The penetration depth of surface plasmon wave is below 200 nm<sup>19</sup> and hence sensed only the refractive index of PTPP substrate because its thickness is larger than 300 nm in the present study.

#### Thickness of the PAAc Layer Prepared on OWS Setup.

To avoid any error caused by the ex-situ sample preparation for the OWS measurements, the UV-induced graft polymerization of AAc was performed in situ directly within the OWS setup (Figure 2). Using this instrument and a PTPP/Au/LaSFN9 substrate mounted to the OWS, the kinetics of the graft polymerization reaction was investigated in situ. A UV spot light source was employed to initiate the graft polymerization reaction. The effect of the AAc concentration and of the UV intensity on the thickness of the grafted PAAc layer was examined. The OWS spectra were recorded before and after UV irradiation. Figure 5 shows the thickness of the grafted PAAc layer as a function of the AAc monomer concentration. The thickness of the PAAc layer increased almost linearly with increasing monomer concentration. This is in good agreement with the previous analysis of the relationship between the AAc concentration and the surface concentration of grafted carboxylic groups.<sup>12</sup> The UV intensity also significantly affected the efficiency of the graft polymerization, as shown in Figure 6. With increasing UV intensity from 160 to 460 and 800 mW/cm<sup>2</sup>, the thickness of the PAAc layer increased from  $d = 225$  to  $d = 274$  and  $d = 324$  nm, respectively. It was reported that the higher UV intensity leads to higher degree of grafting,<sup>3,4</sup> thus resulting in a higher thickness.

The thickness and the refractive index of the PAAc layer are sensitive to the pH value of the aqueous medium.<sup>16,25,26</sup> At a

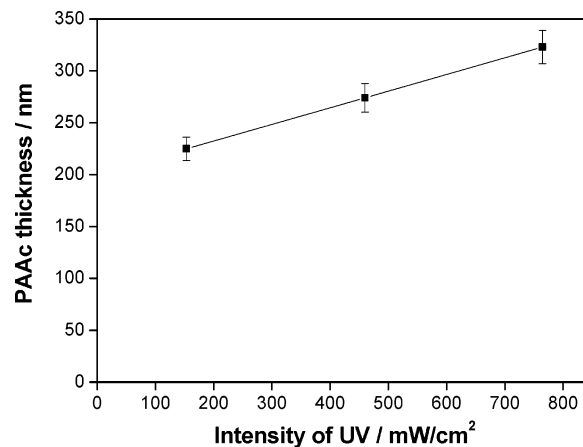


**Figure 6.** Effect of the UV intensity on the thickness of grafted PAAc layer prepared in the OWS setup. The PAAc layer is in contact with aqueous AAc solution. Grafting conditions: 5% AAc, 10 min.

pH higher than the  $pK_a$  of the poly(acrylic acid), the COOH groups along PAAc chains are dissociated to COO<sup>−</sup>, which leads to electrostatic repulsion within the PAAc chain, resulting in a more extended configuration of the grafted chains. At pH = 2, the thickness of the PAAc layer (at 1% AAc; UV: 460 mW/cm<sup>2</sup>) was found to be  $d = 654$  nm and  $n = 1.471$ . If the pH of the aqueous solution was increased to pH = 10, the thickness increased to  $d = 676$  nm, while the refractive index decreased to  $n = 1.468$ , as expected. The results suggest that the PAAc layer prepared by UV-induced graft polymerization shows properties of a polymer brush.

**Thickness of the PAAc Layer Loaded with Galactose Ligands.** The carboxylic groups on the grafted PAAc chains were utilized to immobilize various biomolecules through covalent linkages. Previously, we have conjugated galactose ligands to carboxylic groups on grafted PAAc chains for liver tissue engineering applications.<sup>12,13</sup> The thickness of the galactosylated PAAc layer in the dry state and in PBS buffer was characterized by OWS (Figure 7). The fitting results are summarized in Table 2. The thickness of the galactosylated layer in the dry state ( $d = 460$  nm) is about 2.5-fold higher than the original PAAc layer ( $d = 182$  nm). Moreover, the refractive index of the galactosylated layer is  $n = 1.533$ , which is higher than the original PAAc layer ( $n = 1.528$ ). Our previous data suggested that the galactosylation was nearly complete due to the large excess of the galactose ligand and coupling reagent (EDC) and the extended reaction time.<sup>12</sup> This high degree of galactosylation likely increases the packing density of the graft chain, thus causing the grafted chains to stretch more, therefore showing a higher thickness than the PAAc layer in the dry state.

In PBS buffer, the thickness of the galactosylated layer ( $d = 951$  nm) is slightly lower than the initial PAAc itself ( $d = 1030$  nm). Because of the coupling of galactose ligands into the PAAc layer, the refractive index of the galactosylated layer in PBS ( $n = 1.466$ ) is higher than that for the original PAAc layer ( $n = 1.429$ ), as indicated in Table 2. The galactosylation of PAAc chains is nearly complete under this condition.<sup>12</sup> Therefore, the galactosylated PAAc chains are not ionizable and not charged, thus showing a low swellability in the aqueous environment. The increase in thickness is solely due to the hydration of the grafted chains as a result of large amount of hydrogen bonds formed between hydroxyl groups in the galactose residues and the water molecules. Therefore, galactosylated surfaces exhibit a lower thickness compared to the PAAc graft layer even through more molecules were incorporated into the layer. The influence of water solubility for the structure of graft chain was

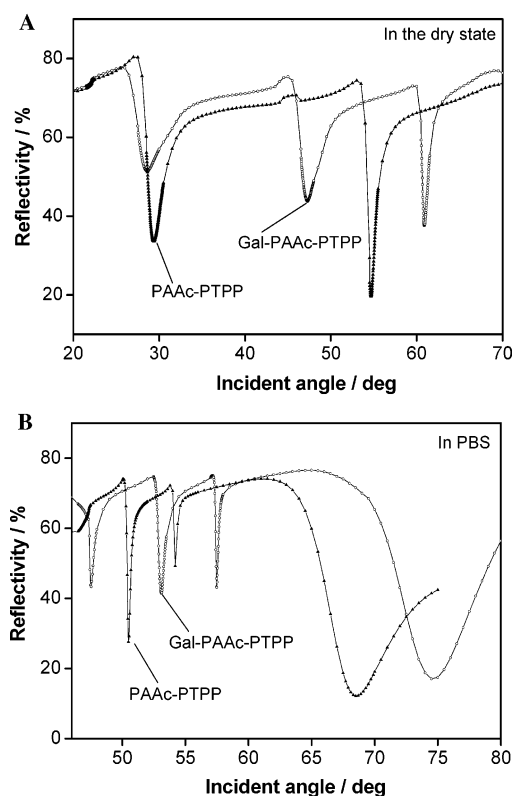


**Figure 7.** p-Polarized OWS spectra of a PAAc-PTPP (▲) and a Gal-PAAc-PTPP layer (○): (A), in the dry state; (B) in PBS buffer.

**Table 2. Thickness and Refractive Index of the PAAc Graft Layer and the Gal-PAAc Layer in the Dry State and in PBS Buffer**

|          | in the dry state |                  | in PBS buffer  |                  |
|----------|------------------|------------------|----------------|------------------|
|          | thickness (nm)   | refractive index | thickness (nm) | refractive index |
| PAAc     | 182              | 1.528            | 1030           | 1.429            |
| Gal-PAAc | 460              | 1.533            | 951            | 1.466            |

also observed previously.<sup>17</sup> On the basis of these findings, a structure model for the grafted PAAc and the Gal-PAAc layers is proposed, as shown in Figure 8. The grafted PAAc layer exhibits an extended conformation in PBS buffer solution

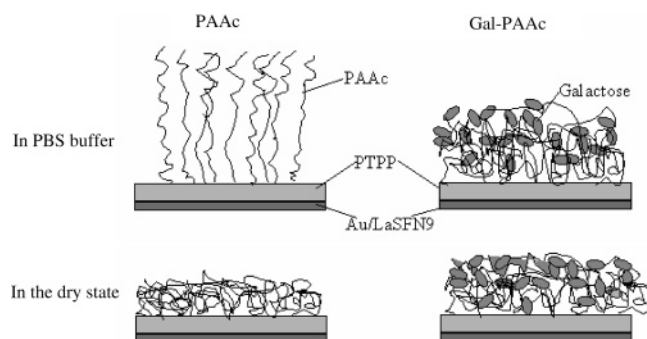


**Figure 8.** Schematic representation of the structure of a grafted PAAc layer and a Gal-PAAc layer in different environments.

(Figure 8, top left). After coupling with galactose ligand, the dry thickness of the Gal-PAAc layer (Figure 8, bottom right) becomes higher than that of the PAAc layer (Figure 8, bottom left). On the other hand, as discussed above, the Gal-PAAc layer in solution (Figure 8, top right) shows lower thickness than the PAAc.

## Conclusions

OWS was utilized to measure the thickness of UV-grafted PAAc layers in the dry state and in aqueous solution. The PAAc layer exhibits properties of a polymer brush. The PAAc chains stretch away in aqueous media and show an increase in thickness at high pH due to the presence of electrostatic repulsion between the COO<sup>-</sup> groups. Higher AAc monomer concentrations and increased UV intensity lead to thicker graft layers. Delamination of the grafted layer from the metal substrate was observed for thicker layers in aqueous media. A structural model for the PAAc graft layer and the galactosylated PAAc layer was proposed. This study demonstrates the unique advantage of OWS for the analysis of surface-grafted polymer chains, particularly in different environments.

## References and Notes

- (1) Kato, K.; Uchida, E.; Kang, E. T.; Uyama, Y.; Ikada, Y. *Prog. Polym. Sci.* **2003**, *28*, 209–259.
- (2) Uyama, Y.; Kato, K.; Ikada, Y. In *Grafting/Characterization Techniques/Kinetic Modeling*; Springer: Berlin, 1998; Vol. 137, pp 1–39.
- (3) Pieracci, J.; Crivello, J. V.; Belfort, G. *Chem. Mater.* **2002**, *14*, 256–265.
- (4) Taniguchi, M.; Pieracci, J.; Samsonoff, W. A.; Belfort, G. *Chem. Mater.* **2003**, *15*, 3805–3812.
- (5) Ma, H. M.; Davis, R. H.; Bowman, C. N. *Macromolecules* **2000**, *33*, 331–335.
- (6) Luo, N.; Hutchison, J. B.; Anseth, K. S.; Bowman, C. N. *Macromolecules* **2002**, *35*, 2487–2493.
- (7) Uchida, E.; Uyama, Y.; Ikada, Y. *J. Appl. Polym. Sci.* **1990**, *41*, 677–687.
- (8) Uchida, E.; Uyama, Y.; Ikada, Y. *J. Polym. Sci., Part A: Polym. Chem.* **1989**, *27*, 527–537.
- (9) Zangmeister, R. A.; Tarlov, M. *J. Langmuir* **2003**, *19*, 6901–6904.
- (10) Li, Z. F.; Ruckenstein, E. *Nano Lett.* **2004**, *4*, 1463–1467.
- (11) Uchida, E.; Uyama, Y.; Ikada, Y. *J. Appl. Polym. Sci.* **1993**, *47*, 417–424.
- (12) Ying, L.; Yin, C.; Zhuo, R. X.; Leong, K. W.; Mao, H. Q.; Kang, E. T.; Neoh, K. G. *Biomacromolecules* **2003**, *4*, 157–165.
- (13) Chua, K. N.; Lim, W. S.; Zhang, P. C.; Lu, H. F.; Wen, J.; Ramakrishna, S.; Leong, K. W.; Mao, H. Q. *Biomaterials* **2005**, *26*, 2537–2547.
- (14) Uchida, E.; Ikada, Y. *Macromolecules* **1997**, *30*, 5464–5469.
- (15) Uchida, E.; Iwata, H.; Ikada, Y. *Polymer* **2000**, *41*, 3609–3614.
- (16) Sarkar, D.; Somasundaran, P. *Langmuir* **2004**, *20*, 4657–4664.
- (17) Uchida, E.; Uyama, Y.; Ikada, Y. *Langmuir* **1994**, *10*, 1193–1198.
- (18) Knoll, W. In *Handbook of Optical Properties II Optics of Small Particles, Interfaces, and Surfaces*; Hummel, R. E., Wissmann, P., Eds.; CRC Press: Boca Raton, FL, 1997; pp 373–400.
- (19) Knoll, W. *Annu. Rev. Phys. Chem.* **1998**, *49*, 569–638.
- (20) Biesalski, M.; Johannsmann, D.; Rühle, J. *J. Chem. Phys.* **2002**, *117*, 4988–4994.
- (21) Biesalski, M.; Rühle, J. *Langmuir* **2000**, *16*, 1943–1950.
- (22) Yin, C.; Ying, L.; Zhang, P. C.; Zhuo, R. X.; Kang, E. T.; Leong, K. W.; Mao, H. Q. *J. Biomed. Mater. Res. A* **2003**, *67A*, 1093–1104.
- (23) Mao, H. Q.; Shipanova-Kadiyala, I.; Zhao, Z.; Dang, W. B.; Brown, A.; Leong, K. W. *J. Biomater. Sci., Polym. Ed.* **2005**, *16*, 135–161.
- (24) Raether, H. *Surface Plasmons on Smooth and Rough Surfaces and on Gratings*; Springer-Verlag: Berlin, 1988.
- (25) Iwata, H.; Hirata, I.; Ikada, Y. *Macromolecules* **1998**, *31*, 3671–3678.
- (26) Ulbricht, M.; Riedel, M. *Biomaterials* **1998**, *19*, 1229–1237.

MA0605620